

Design of LPV-PI-like controller with guaranteed performance for discrete-time systems under saturating actuators[★]

Larissa S. Figueiredo^{*} Tárzis A. R. Parreiras^{***}
Márcio J. Lacerda^{*,**} Valter J. S. Leite^{*,***}

^{*} Graduate Program in Electrical Engineering - CEFET / MG & UFSJ
(e-mail: larissasoaes21@outlook.com, valter@ieee.org).

^{**} Department of Electrical Engineering / Federal University of São
João del-Rei (UFSJ) (e-mail: lacerda@ufsj.edu.br)

^{***} Department of Mechatronics Engineering / CEFET-MG / campus
Divinópolis (e-mail: tarsis1544@hotmail.com, valter@ieee.org)

Abstract: This paper presents new conditions to design linear parameter-varying (LPV) state-feedback controllers for systems under saturating actuators. The proposed design ensures a minimal rate of contractivity of an associated Lyapunov function. A proportional-integral (PI) like structure is employed to ensure null tracking error for piecewise constant reference signals. Therefore, this proposal fits the design requirements of LPV and quasi-LPV real systems under saturating actuators. Experimental essays conducted on a second-order nonlinear level control illustrate the potential of the proposed approach. Additionally, the tests indicate how the contractivity rate affects the size of the estimate of the region of attraction.

Keywords: LPV controller, quasi-LPV systems, PI like controller, saturating actuators.

1. INTRODUCTION

Linear parameter-varying (LPV) models are used to describe with high fidelity complex dynamics systems or those requiring high performance. These LPV systems have a time-varying parameter vector that modifies their dynamic behavior. Quasi-LPV and quasi-NLPV systems are more general cases of LPV ones, where the parameter vector is calculated from some available measures on the system (such as output or state of the system), while in LPV systems the parameter is measured directly (Grimble, 2018). NLPV models may lead to high fidelity representations with the time-varying parameters appearing nonlinearly (Blesa et al., 2014).

Many real systems exhibit dynamics that can be better described by LPV models. Moreover, there is a growing interest in this modeling structure in several areas, such as automotive systems (Yamamoto et al., 2019), energy (Morato et al., 2020), among others. When considering LPV systems, parameter-dependent controllers and filters can achieve higher performance than robust structures (Sename et al., 2019; Lacerda et al., 2016). A quite common approach consists in using the Lyapunov method to design LPV controllers (Briat, 2014). The advantage of using this method is that we can usually obtain convex conditions formulated in terms of Linear Matrix Inequalities (LMIs).

In real systems, the magnitude of the control signal should be limited, either for physical or safety reasons. However,

^{*} Authors thank the financial support from CEFET-MG and the Brazilian agency CNPq, grant 311208/2019-3.

this limitation may cause undesirable effects in the system, such as limit cycles, parasitic equilibrium points, and even lead the closed-loop to instability, thus justifying the study of saturating actuators (Tarbouriech et al., 2011). For these reasons, it is necessary to characterize the region of attraction of the system to find a set of admissible initial states, such that the trajectories starting in such a set converge to the origin, assuring the local stability of LPV systems (Binazadeh and Bahmani, 2017; Ruiz et al., 2019) and quasi-LPV systems (Lopes et al., 2018).

This paper presents a new convex procedure to design LPV controllers with a proportional action over the state of the system and an integral action over the tracking error. The Lyapunov function and both gains are parameter-dependent. Additionally, our proposal can ensure performance to the closed-loop systems by ensuring a rate of contractivity of the Lyapunov function. We illustrate the application of our design method in nonlinear second-order coupled tanks, modeled as a quasi-LPV system. We run four real-time essays, two for reference tracking, and two for disturbance rejection. We explore different saturation levels, showing the efficacy of the proposal.

Notation: The symbol \star represents a symmetric block in the LMIs. Identity and zero matrices are represented by \mathbf{I} and $\mathbf{0}$, respectively. The set of real numbers is denoted by \mathbb{R} . $M \in \mathbb{R}^{n \times n_u}$ is matrix of dimension $n \times n_u$ with real entries and $x \in \mathbb{R}^n$ is a vector with n positions and real entries. $\text{He}(M) = M + M^T$. The term $\text{diag}\{X, U\}$ is equivalent to a block diagonal matrix, i.e., $\begin{bmatrix} X & 0 \\ 0 & U \end{bmatrix}$.

2. PROBLEM FORMULATION

Consider the time-varying discrete-time linear system subject to saturating actuators described by:

$$\begin{aligned} x_{k+1} &= A(\alpha_k)x_k + B(\alpha_k)\text{sat}(u_k), \\ y_k &= Cx_k, \end{aligned} \quad (1)$$

where $x_k \in \mathbb{R}^n$ is the state vector, $u_k \in \mathbb{R}^{n_u}$ is the control input, $\text{sat}(u_k)$ is the symmetric saturation function given by $\text{sat}(u_{k,(r)}) = \text{sign}(u_{k,(r)}) \min(|u_{k,(r)}|, \rho_{(r)})$, $r = 1, \dots, n_u$, $\rho \in \mathbb{R}^{n_u}$, $\rho_{(r)}$ is the maximum allowed amplitude of $u_{k,(r)}$ due to the actuator saturation, and $C \in \mathbb{R}^{n_y \times n}$ is the output matrix. Due to the presence of saturating actuators, the local stability approach is required. The linear parameter-dependent matrices of the dynamic equation (1), $A(\alpha_k) \in \mathbb{R}^{n \times n}$ and $B(\alpha_k) \in \mathbb{R}^{n \times n_u}$, belong to a polytopic domain given by the convex combination of N known vertices:

$$[A(\alpha_k), B(\alpha_k)] = \sum_{i=1}^N \alpha_{k,i} [A_i, B_i], \quad (2)$$

where $\alpha_k \in \Lambda$ is the known vector of the time-varying parameters verifying the unit simplex Λ :

$$\Lambda = \left\{ \alpha_k \in \mathbb{R}^N : \sum_{i=1}^N \alpha_{k,i} = 1, \alpha_{k,i} \geq 0, i = 1, \dots, N \right\}. \quad (3)$$

Such a polytopic representation is quite general and often found in LPV context, where α_k concerns the measured parameter (Briat, 2014).

The objective of this work is to design a parameter-dependent proportional-integral (PI) action, based on state feedback controller, for the system (1)-(3). The controller is designed to ensure null steady-state error for piecewise constant references. The error is given by

$$e_k = r_k - y_k, \quad (4)$$

where r_k is the desired output of the system. Fig. 1 depicts the topology of the controller to be designed in this work. The closed-loop system has order greater than system (1)

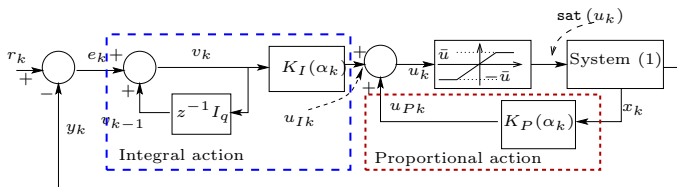


Fig. 1. Topology of an integral action state feedback LPV controller.

because of the integral action. By defining an augmented state vector $\xi_k = [x_k^T \ v_k^T]^T$, the closed-loop system shown in Fig. 1 can be rewritten as

$$\begin{aligned} \xi_{k+1} &= \mathcal{A}(\alpha_k)\xi_k + \mathcal{B}(\alpha_k)\text{sat}(u_k), \\ y_k &= \mathcal{C}\xi_k, \end{aligned} \quad (5)$$

with $\mathcal{C} = \begin{bmatrix} C^T \\ \mathbf{0} \end{bmatrix}^T$, $\mathcal{A}(\alpha_k) = \begin{bmatrix} A(\alpha_k) & \mathbf{0} \\ -CA(\alpha_k) & \mathbf{I} \end{bmatrix}$, $\mathcal{B}(\alpha_k) = \begin{bmatrix} B(\alpha_k) \\ -CB(\alpha_k) \end{bmatrix}$. A control law for system (5) is proposed as

$$u_k = K(\alpha_k)\xi_k, \quad K(\alpha_k) = [K_P(\alpha_k) \ K_I(\alpha_k)], \quad (6)$$

with $K(\alpha_k) = \sum_{i=1}^N \alpha_{k,i} K_i$. Moreover, to handle the non-linearity $\text{sat}(u_k)$, the dead-zone function $\Psi(u_k)$ will be employed

$$\Psi(u_k) = u_k - \text{sat}(u_k). \quad (7)$$

By considering (6)-(7), we rewrite the closed-loop system (5) as

$$\xi_{k+1} = \mathcal{A}_{cl}(\alpha_k)\xi_k - \mathcal{B}(\alpha_k)\Psi(u_k), \quad (8)$$

where $\mathcal{A}_{cl}(\alpha_k) = \mathcal{A}(\alpha_k) + \mathcal{B}(\alpha_k)K(\alpha_k)$ is the closed loop dynamic matrix.

We use the generalized sector condition proposed by Gomes da Silva Jr. and Tarbouriech (2005) to deal with the dead zone function. Also, the set \mathbb{S} is defined as

$$\mathbb{S}(u_k - d_k, \rho) = \{ \xi \in \mathbb{R}^{n+1} : |[K_{(r)}(\alpha_k) - G_{(r)}(\alpha_k)] \xi_k| \leq \rho_{(r)} \}, \quad (9)$$

$r = 1, \dots, n_u$, with the auxiliary signal $d_k = G(\alpha_k)\xi_k$ used as a degree of freedom in the design conditions.

Due to the saturating actuators, only initial conditions in a subset of \mathbb{R}^{n+1} yield the trajectories of (5)-(6) to converge to the origin. Such a subset is denoted by $\mathcal{R}_A \subseteq \mathbb{R}^n$, being called the region of attraction or basin of attraction. The determination of \mathcal{R}_A is not an easy task even for small order systems since it can be non-convex, open, and in some cases, unbounded (Tarbouriech et al., 2011). Therefore, an estimate of the region of attraction $\mathcal{R}_E \subseteq \mathcal{R}_A$ is computed, usually the largest possible. One way to construct the \mathcal{R}_E estimate is to employ level sets taken from the Lyapunov function associated with the closed-loop system. To this end, a quadratic parameter-dependent Lyapunov function is considered:

$$V(\xi_k, \alpha_k) = \xi_k^T P(\alpha_k) \xi_k, \quad P(\alpha_k) = \sum_{i=1}^N \alpha_{i,k} P_i > 0. \quad (10)$$

From (Daafouz and Bernussou, 2001a), if there exist a function given by (10) fulfilling the Lyapunov conditions for stability of (5)-(6), then we say that such a system is polyquadratic stable. In such a case, a level set associated with the Lyapunov function can be defined as in the following lemma.

Lemma 1. Suppose that $V(\xi_k, \alpha_k)$ given in (10) is a Lyapunov function for system (5)-(6). Then, a possible level set is given by

$$\mathcal{L}_V(\mu) = \bigcap_{\alpha_k \in \Lambda} \mathcal{E}(P(\alpha_k), \mu) = \bigcap_{i=1}^N \mathcal{E}(P_i, \mu) \quad (11)$$

for $\mu > 0$ and

$$\mathcal{E}(P_i, \mu) = \{ \xi(k) \in \mathbb{R}^n; \xi_k^T P_i \xi_k \leq \mu \}. \quad (12)$$

For the proof, see of this lemma can be found in (Jungers and Castelan, 2011).

Observe that, when the time-varying parameters α_k in (1) are computed from other measured variables, for instance, the output of the system, then, the system is called a quasi-LPV system. An example of such system can be found in the Takagi-Sugeno approach, where α_k can be analytically computed from the states of the system. Another example is given in Section 4, where the values of α_k are computed from the measured output of the system.

$$\begin{bmatrix} \text{He}(X_{11,i}) - \lambda Q_{11,i} & X_{12,i} + X_{21,i}^T - \lambda Q_{12,i} & -W_{11,i}^T & X_{11,i}^T A_i^T & -X_{11,i}^T A_i^T C^T + X_{21,i}^T & -L_{11,i}^T \\ X_{21,i} + X_{12,i}^T - \lambda Q_{21,i} & \text{He}(X_{22,i}) - \lambda Q_{22,i} & -W_{12,i}^T & X_{12,i}^T A_i^T & -X_{12,i}^T A_i^T C^T + X_{22,i}^T & -L_{12,i}^T \\ \star & \star & \text{He}(V_{11,i}) & -V_{11,i}^T B_i^T & V_{11,i}^T B_i^T C^T & \mathbf{0} \\ \star & \star & \star & Q_{11,j} - R_{11,ij} & Q_{12,j} - R_{12,ij} & B_i Z_{11,j} - Y_{11,j}^T \\ \star & \star & \star & \star & Q_{22,j} - R_{22,ij} & -CB_i Z_{11,j} - Y_{12,j}^T \\ \star & \star & \star & \star & \star & Z_{11,j} + Z_{11,j}^T \end{bmatrix} > \mathbf{0} \quad (13)$$

3. MAIN RESULTS

The following theorem presents conditions for the stabilization of system (5) under the effect of λ -contractivity and assuming the control law (6). Our approach is inspired by the recent work of Pandey and de Oliveira (2017), where the LMI conditions proposed in (Daafouz and Bernussou, 2001b) for polyquadratic stabilization were generalized to consider time-varying input matrix.

Theorem 2. Consider the saturating LPV discrete-time system given by (5) and a scalar $\lambda \in]0, 1]$. Suppose that there exist positive-definite matrices $Q_i = Q_i^T \in \mathbb{R}^{(n+1) \times (n+1)}$, diagonal positive-definite matrices $V_i \in \mathbb{R}^{(n_u+1) \times (n_u+1)}$, matrices $X_i \in \mathbb{R}^{(n+1) \times (n+1)}$, $L_i \in \mathbb{R}^{(n_u+1) \times (n+1)}$, $Y_j \in \mathbb{R}^{(n_u+1) \times (n+1)}$, $Z_j \in \mathbb{R}^{(n_u+1) \times (n_u+1)}$, $W_i \in \mathbb{R}^{(n_u+1) \times (n+1)}$, $i, j = 1, \dots, N$, such that the LMIs (13) (top of this page) and

$$\begin{bmatrix} -\rho_{(r)}^2 & L_{11,i(r)} - W_{11,i(r)} & L_{12,i(r)} - W_{12,i(r)} \\ \star & Q_{11,i} - \text{He}(X_{11,i}) & Q_{12,i} - X_{12,i} - X_{21,i}^T \\ \star & Q_{21,i} - X_{21,i} - X_{12,i}^T & Q_{22,i} - \text{He}(X_{22,i}) \end{bmatrix} < \mathbf{0} \quad (14)$$

with

$$R_{ij} = \text{He} \left(\begin{bmatrix} B_i Y_{11,j} & B_i Y_{12,j} \\ -CB_i Y_{11,j} & -CB_i Y_{12,j} \end{bmatrix} \right), \quad (15)$$

$\forall i, j = 1, \dots, N$, and $r = 1, \dots, n_u$, are satisfied. Then, the parameter-dependent control gain

$$K_i = [L_{11,i} \ L_{12,i}] \begin{bmatrix} X_{11,i} & X_{12,i} \\ X_{21,i} & X_{22,i} \end{bmatrix}^{-1} \quad (16)$$

$i = 1, \dots, N$, where $K_i = [K_{P,i} \ K_{I,i}]$, with control law (6), locally and polyquadratically stabilizes the resulting closed-loop system for all initial conditions belonging to the set $\mathcal{R}_{\mathcal{E}} = \mathcal{L}_{\mathcal{V}}(1)$.

Proof. By assuming (13) holds, we replace $[L_{11,i} \ L_{12,i}]$ and $[W_{11,i} \ W_{12,i}]$ by $[K_{P,i} X_{11,i} + K_{I,i} X_{21,i} \ K_{P,i} X_{12,i} + K_{I,i} X_{22,i}]$ and $[G_{11,i} X_{11,i} + G_{12,i} X_{21,i} \ G_{11,i} X_{12,i} + G_{12,i} X_{22,i}]$, respectively, and we use the known fact for matrix $R > \mathbf{0}$ and M we have $(M-R)R^{-1}(M-R)^T \geq \mathbf{0} \Rightarrow MR^{-1}M^T \geq -R + M + M^T$, to overbound the block (1, 1) of the resulting inequality. Next, by pre- and post-multiplying the resulting condition by $\text{diag}\left\{ \begin{bmatrix} X_{11,i} & X_{12,i} \\ X_{21,i} & X_{22,i} \end{bmatrix}^{-T}, \mathbf{I}, \mathbf{I}, \mathbf{I} \right\}$, and its transpose, respectively, and defining $H_i = Z_{11,i}^{-T}$,

$$P_i = \begin{bmatrix} Q_{11,i} & Q_{12,i} \\ \star & Q_{22,i} \end{bmatrix}^{-1}, \quad F_i = \begin{bmatrix} P_{11,i} & P_{12,i} \\ \star & P_{22,i} \end{bmatrix} \begin{bmatrix} Y_{11,j} \\ Y_{21,j} \end{bmatrix}^T H_{11,i},$$

for all $i, j = 1, \dots, N$, we get (17) (see top of the next page), with R_{ij} given by (15), which can be rewritten as

$$R_{ij} = \text{He} \left(\begin{bmatrix} B_i \\ -CB_i \end{bmatrix} H_{11,j}^{-T} \begin{bmatrix} F_{11,j} & F_{21,j} \\ \star & P_{22,j} \end{bmatrix} \begin{bmatrix} P_{11,j} & P_{12,j} \\ \star & P_{22,j} \end{bmatrix}^{-1} \right),$$

for all $i, j = 1, \dots, N$. By pre- and post-multiplying (17)

by $\text{diag}\left\{ \mathbf{I}, V_{11,i}^{-T}, \begin{bmatrix} \mathbf{0} & \mathbf{0} & H_{11,j} \\ P_{11,j} & P_{12,j} & F_{11,j} \\ \star & P_{22,j} & F_{21,j} \end{bmatrix} \right\}$ and its transpose, respectively, and due the regularity of V_i , replacing $S_i = V_{11,i}^{-1}$, we can multiply the resulting inequality by α_i , α_j , $\alpha \in \Lambda$, and summing them up for $i, j = 1, \dots, N$, and pre- and post-multiply the result by

$$\begin{bmatrix} \mathbf{0} & \mathbf{0} & \mathbf{0} & P(\alpha_{k+1})^{-1} \\ \mathbf{I} & \mathbf{0} & \begin{bmatrix} K_P(\alpha_k)^T \\ K_I(\alpha_k)^T \end{bmatrix} & \mathbf{0} \\ \mathbf{0} & \mathbf{I} & \mathbf{0} & \mathbf{0} \end{bmatrix}$$

and its transpose, respectively, to get a parameter-dependent inequality. After, apply Schur's complement and pre- and post-multiplying the resulting inequality by $[\xi_k^T \ \Psi(u_k)^T]$ and its transpose, to rewrite it as $\xi_{k+1}^T P(\alpha_{k+1}) \xi_{k+1} - \xi_k^T \lambda P(\alpha_k) \xi_k - 2\Psi(K(\alpha_k) \xi_k)^T S(\alpha_k) (\Psi(K(\alpha_k) \xi_k) - G(\alpha_k) \xi_k) < 0$ with $K(\alpha_k)$ in (6),

$$P(\alpha_k) = \begin{bmatrix} P_{11}(\alpha_k) & P_{12}(\alpha_k) \\ \star & P_{22}(\alpha_k) \end{bmatrix}, \quad G(\alpha_k) = [G_{11}(\alpha_k) \ G_{12}(\alpha_k)]. \quad (18)$$

Suppose $\xi_k \in \mathbb{S}$ (defined in equation (9)); note that, this hypothesis is confirmed later with the aid of (14). Then, take $\underline{\beta}$ as the minimal eigenvalue of P_i , $i = 1, \dots, N$. Similarly, take $\bar{\beta}$ as the maximal eigenvalue of P_i , $i = 1, \dots, N$. Then, we have $\underline{\beta} \|\xi_k\|_2^2 \leq V(\xi_k, \alpha_k) \leq \bar{\beta} \|\xi_k\|_2^2$ and there exists some $\beta > 0$ such that $\Delta V(\xi_k, \alpha_k) = \xi_{k+1}^T P(\alpha_{k+1}) \xi_{k+1} - \xi_k^T \lambda P(\alpha_k) \xi_k \leq -\beta \|\xi_k\|_2^2$, for all $\alpha_k \in \Lambda$. As a consequence, we conclude that system (5) have trajectories such that its Lyapunov function is λ -contractive. Therefore, the feasibility of inequality (13) implies the (local) polyquadratic (Daafouz and Bernussou, 2001a) stabilization of system (1) by a control law (6) with state-feedback gain (16), ensuring a minimal contractivity rate of the Lyapunov function.

Condition (14) ensures that $\mathcal{L}_{\mathcal{V}}(1)$ given in (11) is included in \mathbb{S} defined in (9). Then, if (14) is also satisfied, by using (16), we replace $[L_{11,i} \ L_{12,i}]$ and $[W_{11,i} \ W_{12,i}]$ by $[K_{P,i} X_{11,i} + K_{I,i} X_{21,i} \ K_{P,i} X_{12,i} + K_{I,i} X_{22,i}]$ and $[G_{11,i} X_{11,i} + G_{12,i} X_{21,i} \ G_{11,i} X_{12,i} + G_{12,i} X_{22,i}]$, respectively, and use again the fact $MR^{-1}M^T \geq -R + M + M^T$ to bound the block (2, 2). Pre- and post-multiplying by $\text{diag}\left\{ \mathbf{I}, \begin{bmatrix} X_{11,i} & X_{12,i} \\ X_{21,i} & X_{22,i} \end{bmatrix}^{-T} \right\}$ and its transpose, multiply by α_i , $\alpha \in \Lambda$, and summing them up for $i = 1, \dots, N$, and applying Schur complement, getting $[K(\alpha_k)_{(r)} - G(\alpha_k)_{(r)}]^T \rho_{(r)}^{-2} [K(\alpha_k)_{(r)} - G(\alpha_k)_{(r)}] - P(\alpha_k) \leq \mathbf{0}$, $\forall \alpha_k \in \Lambda$ and $r = 1, \dots, n_u$. Pre- and post-multiply the last inequality by ξ_k^T and its transpose, respectively, yields $\xi_k^T [K(\alpha_k)_{(r)} - G(\alpha_k)_{(r)}]^T \rho_{(r)}^{-2} [K(\alpha_k)_{(r)} - G(\alpha_k)_{(r)}] \xi_k -$

$$\begin{bmatrix} \lambda P_{11,i} & \lambda P_{12,i} & -G_{11,i}^T \\ \star & \lambda P_{22,i} & -G_{12,i}^T \\ \star & \star & \text{He}(V_{11,i}) \end{bmatrix} \begin{bmatrix} A_i^T & -A_i^T C \\ \mathbf{0} & \mathbf{I} \\ -V_{11,i}^T B_i^T & V_{11,i}^T B_i^T C^T \end{bmatrix} \begin{bmatrix} -K_{P,i}^T \\ -K_{I,i}^T \\ \mathbf{0} \\ B_i H_j^T - P_j^{-1} F_j H_j^{-1} \\ H_j^{-1} + H_j^{-T} \end{bmatrix} > 0 \quad (17)$$

$\xi_k^T P(\alpha_k) \xi_k \leq 0$ for all $\alpha_k \in \Lambda$ and $r = 1, \dots, n_u$, where $K(\alpha_k)$ given in (6), and $G(\alpha_k)$ and $P(\alpha_k)$ given in (18). Consequently, the set \mathcal{S} includes the contractive set $\mathcal{R}_{\mathcal{E}} = \mathcal{L}_{\mathcal{V}}(1)$. As a result, the LPV closed-loop system subject to saturating actuators (1) and control law (6) with state-feedback gain (16), has its trajectories emanating from $\mathcal{R}_{\mathcal{E}}$ converging to the origin without leaving $\mathcal{R}_{\mathcal{E}}$.

3.1 Optimization design procedures

We consider the procedure of maximizing an ellipsoid given by $\mathcal{E}(H)$, $H \in \mathbb{R}^{(n+1) \times (n+1)}$, internal to the ellipsoids determined by $\mathcal{E}(P_i)$, $\forall i = 1, \dots, N$. Thus, we have:

$$\mathcal{P}_H \equiv \begin{cases} \min_{Q_i, X_i, L_i, Y_i, Z_i} \text{trace}(H) \\ \text{subject to: LMIs (13), (14) and} \\ \begin{bmatrix} \begin{bmatrix} Q_{11,i} & Q_{12,i} \\ \star & Q_{22,i} \end{bmatrix} & \mathbf{I} \\ \mathbf{I} & \begin{bmatrix} H_{11} & H_{12} \\ \star & H_{22} \end{bmatrix} \end{bmatrix} \geq 0, \end{cases} \quad (19)$$

for all $i = 1, \dots, N$.

Thus, due to Theorem 2, this optimization procedure allows saturating control signal, yielding more aggressive control actions.

4. EXPERIMENTAL RESULTS

We illustrate our proposal with a second-order nonlinear level process modeled by a quasi-LPV model. The process consists of two coupled tanks with standard industrial sensors and actuators. In the sequel, we present the experimental setup, followed by the physical modeling, and lastly, the experimental achievements.

4.1 Experiment Setup

The tests are made on a plant using two cylindrical tanks, TQ-01 and TQ-02, each of them with 200 l capacity and 0.7 m height, actuated by a 1 hp pump with variable velocity. The output flow rate of the tank TQ-01 goes to a reservoir that supports 400 l, utilized by the pump to recirculate the water to the tank TQ-02. The level must be controlled in the tank TQ-01, where a nonlinear solid designed in expanded polystyrene was put inside. Fig. 2 shows the schematic of the system.

We program the controller with the aid of a Python-based interface (Sousa et al., 2018) and runs it in a low-cost computer (Raspberry Pi 3) where it is easily programmed. The controller takes the measures performed and stored in a Simatic S7-300 programmable logic controller (PLC) using ethernet communication. The PLC sends the control signal to a WEG CFW09 inverter that commands the pump velocity.

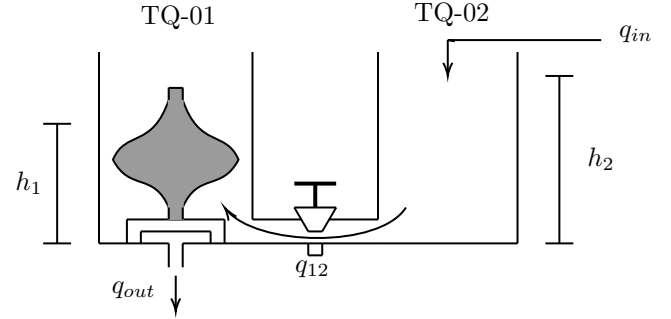


Fig. 2. Schematics of Tank System

4.2 Modeling

We model the system by applying mass balance equations on each tank. From experimental data, we have the following equations modeling the flow to TQ-02 (q_{in}), between TQ-02 and TQ-01 (q_{12}), and from TQ-01 to the reservoir (q_{out}): $q_{in} = (1.64u + 35.7) \times 10^{-5}$, $q_{12} = (33.5(h_2(t) - h_1(t)) + 4.31) \times 10^{-4}$, $q_{out} = (8.71\sqrt{h_1(t)} + 3.1) \times 10^{-4}$, where $0\% \leq u \leq 100\%$ is the control signal, $h_1(t)$ and $h_2(t)$ the level on tanks TQ-01 and TQ-02, respectively. Thus, we have for tank TQ-01:

$$\frac{d}{dt} \int_0^{h_1} a(h) dh = q_{12} - q_{out} \quad (20)$$

where q_{12} and q_{out} are the inlet and outlet flows, $a(h_1)$ is the transverse area at level h_1 : $a(h_1(t)) = \frac{3r}{5} \left(2.7r - \frac{\cos(2.5\pi(h_1(t) - \mu))}{\sigma\sqrt{2\pi}} e^{-\frac{(h_1(t) - \mu)^2}{2\sigma^2}} \right)$.

The variable $r = 0.31$ m is the radius of the tank, the parameters $\mu = 0.4$ and $\sigma = 0.55$ are related to the Gaussian profile of the solid. Because of $a(h_1)$, the integral in (20) do not have an analytical expression. We propose to overcome this issue by approximating the terms depending on $\cos(z)$ and e^w by their Taylor's series, with $z = 2.5\pi(h_1(t) - \mu)$ and $w = \frac{-(h_1(t) - \mu)^2}{2\sigma^2}$. The number of terms was chosen to ensure $|a(h_1) - \tilde{a}(h_1)| \leq 4 \times 10^{-3}$.

$$\tilde{a}(h_1(t)) = \frac{3r}{5} \left(2.7r - \frac{1}{\sigma\sqrt{2\pi}} \left(1 - \frac{z^2}{2} - \frac{z^4}{720} - \frac{z^6}{720} + \frac{z^8}{40320} \right) \left(1 + w + \frac{w^2}{2} - \frac{w^3}{6} + \frac{w^4}{24} \right) \right) \quad (21)$$

Replacing $a(h_1)$ by $\tilde{a}(h_1)$ in (20), it is possible to get:

$$\dot{h}_1(t) = \frac{q_{12} - q_{out}}{\tilde{a}(h)} \quad (22)$$

which models the level dynamics in tank TQ-01. For the tank TQ-02, the cross area is constant and equals to 0.3019 m², which, by similar steps done for TQ-01, yields:

$$\dot{h}_2(t) = \frac{q_{in} - q_{12}}{0.3019} \quad (23)$$

Therefore, the nonlinear model given by (22)-(23) model the dynamics of the couple tanks.

We highlight that the obtained model depends on the measured levels. In particular, the area $\tilde{a}(h_1)$ depends on the height of TQ-01, which is measured. Therefore, the system fits in a system quasi-LPV, i.e., a system that depends on a parameter that is obtained indirectly from other measurements taken online.

Because of the maximal height of the tanks, we take the levels in the range of $0.28 \text{ m} \leq h_1(t) \leq 0.48 \text{ m}$. For such a range, it is possible to envelop the dynamics by two linear models, one at each extreme value of $h_1(t)$. The LPV parameter is then computed by

$$\alpha_1(k) = -0.05h_1 + 2.4. \quad (24)$$

We discretized the continuous-time model with a sample time of $T_s = 5.2632 \text{ s}$, which is about one-fifth of the faster time constant in the operational range, and including the zero-order-holder effect. The matrices of the discretized version of the continuous-time model, computed at the extreme values of $h_1(t)$ yield the vertices matrices:

$$A_1 = \begin{bmatrix} 0.9455 & 0.0540 \\ 0.0752 & 0.9057 \end{bmatrix}, A_2 = \begin{bmatrix} 0.9466 & 0.0528 \\ 0.1130 & 0.8652 \end{bmatrix}, C = \begin{bmatrix} 0 \\ 1 \end{bmatrix}^T, \\ B_1 = \begin{bmatrix} 0.2779 \\ 0.0111 \end{bmatrix} \times 10^{-3}, B_2 = \begin{bmatrix} 0.2780 \\ 0.0167 \end{bmatrix} \times 10^{-3}. \quad (25)$$

4.3 Experimental Results

The gain scheduling demand a choice of the saturation limit ρ and the contractivity constant λ . To illustrate our proposal, we apply the optimization problem (19) to the modeled system for $\rho = 25\%$ and $\rho = 15\%$. The first ρ is the maximal symmetrical control value around the minimal operational condition in the range $0.28 \leq h_1(t) \leq 0.48 \text{ m}$. The second one leads to even constrained values on the actuator. The value of λ affects the size of $\mathcal{R}_{\mathcal{E}}$ directly. The smaller λ , the smaller the region of attraction. If λ is chosen too close to unity, the region $\mathcal{R}_{\mathcal{E}}$ is unrealistic, allowing levels higher than the height of the tanks. On the other hand, small values of λ lead to very fast convergence, but too small regions of attraction. We choose $\lambda = 0.95$, empirically, establishing a compromise between the size of $\mathcal{R}_{\mathcal{E}}$ and the velocity of convergence. So, with $\rho = 25\%$ the optimization problem (19) yields $K_{P1} = [-2.6568 \ -1.6630] \times 10^3$, $K_{I1} = 109.6971$, $K_{P2} = [-2.7894 \ -1.6076] \times 10^3$, $K_{I2} = 111.8418$, and with $\rho = 15\%$ we got $K_{P1} = [-2.7336 \ -1.7116] \times 10^3$, $K_{I1} = 112.9695$, $K_{P2} = [-2.8681 \ -1.6491] \times 10^3$, $K_{I2} = 114.8949$. Because of (24), equation (6) can be rewritten as: $K_P(h_1(t)) = 0.05h_1(t)(K_{P2} - K_{P1}) - 2.4K_{P1} + 1.4K_{P2}$ and $K_I(h_1(t)) = 0.05h_1(t)(K_{I2} - K_{I1}) - 2.4K_{I1} + 1.4K_{I2}$.

With these gains, we performed two kinds of essays: one for reference tracking and another for regulation around a given setpoint.

Reference tracking: For each controller designed, we run a real-time experiment to track a sequence of reference steps. The achieved results are in Fig. 3 where it is clear that both controllers drive the level to the desired value with null off-set. The reader can observe in the detail of this figure that, the design with $\rho = 25\%$ (red dotted line) is more aggressive, leading to a faster time-response, with smaller rise-time. The overshoots of both designs are almost the same, as well as the settling time. In both

designs and for all steps, the controlled output goes to the reference value, as expected. The reader can note in

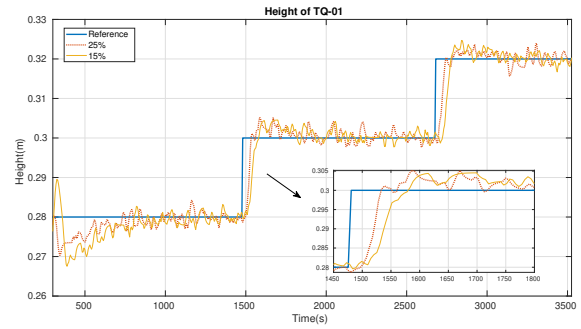


Fig. 3. Level of tank TQ-01, ($h_1(t)$), for the controllers assuming $\rho = 25\%$ (red dotted line) and $\rho = 15\%$ (orange solid line).

Fig. 4 the control signals (blue lines) and the respective saturation limits (red dashed lines). Note that the control uses all the allowed range, achieving saturation in several instants, especially at those corresponding to the reference step.

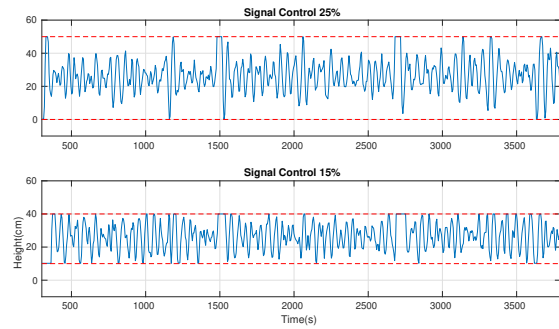


Fig. 4. Control Signals. The red dashed lines represents the control signals bounds and the blue lines the control signals for $\rho = 25\%$ (top) and $\rho = 15\%$ (bottom).

Level regulation: For each controller designed, we run a real-time experiment to keep the level at $h_1(t) = 0.32 \text{ m}$; we show the achieved results in Fig. 5. At $t = 3500 \text{ s}$, a standard disturbance is imposed on the process, raising the controlled level to more than 0.335 m ; see also the zoom, where it is clear that the controller with a larger saturation bound ($\rho = 25\%$) has a slightly more aggressive action driving the controlled level (red dotted line) back to the reference. The control signals act to reject the disturbance achieving the saturation bounds, as shown in Fig. 6. It is clear that in the more constrained control signal ($\rho = 15\%$, bottom plot), the number of times that the actuator saturates is bigger than for the saturation bound $\rho = 25\%$ (top plot). Such difference occurs because both designs share the same contractivity parameter of $\lambda = 0.95$ despite the concerning saturation bounds.

We chose the more severe case, $\rho = 15\%$, to illustrate that the controlled trajectories do not leave the estimated $\mathcal{R}_{\mathcal{E}}$. This case has a smaller region $\mathcal{R}_{\mathcal{E}}$ than the achieved one with $\rho = 25\%$. Therefore, we plot in Fig. 7 the trajectories of both tests (reference tracking and level regulation),

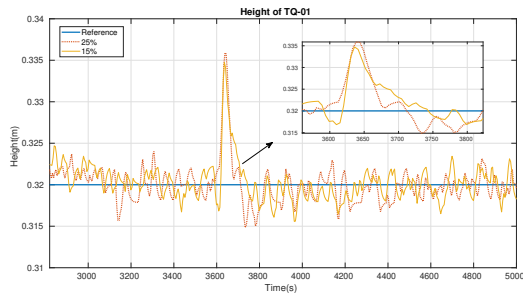


Fig. 5. Level of TQ-01 under disturbance for controllers design with $\rho = 25\%$ (red dotted line) and $\rho = 15\%$ (orange solid line).

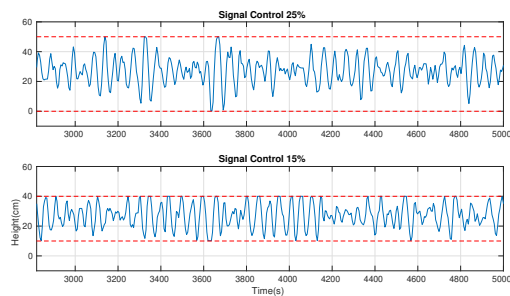


Fig. 6. Control Signals. The dashed lines represents the signals limits

showing that they remain inside $\mathcal{R}_\mathcal{E}$. On the detail, we show a cut of the ellipsoidal sets with the plane $x_I = 0$ and the projection of the trajectories.

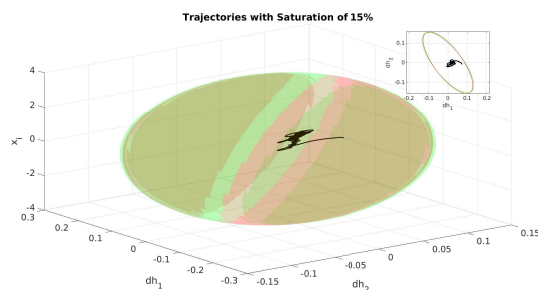


Fig. 7. Estimate $\mathcal{R}_\mathcal{E}$ for $\rho = 15\%$ and the tracking and regulation trajectories (black line).

5. CONCLUSIONS

We presented new convex design conditions for a linear parameter varying proportional-integral (PI) like action. The LPV proportional action comes from state feedback, and the LPV integral-one acts over the tracking error. These conditions ensure the local-polyquadratic stabilization of parameter-dependent processes. We illustrate the proposal with the application to a quasi-LPV level control of a second-order nonlinear system. The real-time experiments show the effectiveness of the design procedure that also ensures a performance index, given by the contractivity of the Lyapunov function.

REFERENCES

- Binazadeh, T. and Bahmani, M. (2017). Design of robust controller for a class of uncertain discrete-time systems subject to actuator saturation. *IEEE Trans. on Automatic Control*, 62(3), 1505–1510.
- Blesa, J., Jiménez, P., Rotondo, D., Nejjari, F., and Puig, V. (2014). An interval nlpv parity equations approach for fault detection and isolation of a wind farm. *IEEE Trans. on Industrial Electronics*, 62(6), 3794–3805.
- Briat, C. (2014). *Linear parameter-varying and time-delay systems*, volume 3. Springer.
- Daafouz, J. and Bernussou, J. (2001a). Parameter dependent Lyapunov functions for discrete-time systems with time-varying parametric uncertainties. *Systems & Control Letters*, 43, 355–359.
- Daafouz, J. and Bernussou, J. (2001b). Parameter dependent Lyapunov functions for discrete time systems with time varying parametric uncertainties. *Systems & Control Letters*, 43(5), 355–359.
- Gomes da Silva Jr., J.M. and Tarbouriech, S. (2005). Antiwindup design with guaranteed regions of stability: an LMI-based approach. *IEEE Trans. on Automatic Control*, 50(1), 106–111.
- Grimble, M.J. (2018). Three degrees of freedom restricted structure optimal control for quasi-LPV systems. In *Proc. of 2018 the IEEE CDC*, 2470–2477. IEEE.
- Jungers, M. and Castelan, E.B. (2011). Gain-scheduled output control design for a class of discrete-time nonlinear systems with saturating actuators. *Systems & Control Letters*, 60(3), 169–173.
- Lacerda, M.J., Tognetti, E.S., Oliveira, R.C.L.F., and Peres, P.L.D. (2016). A new approach to handle additive and multiplicative uncertainties in the measurement for \mathcal{H}_∞ LPV filtering. *Int. J. of Systems Science*, 47(5), 1042–1053.
- Lopes, A.N.D., Leite, V.J.S., and Silva, L.F.P. (2018). On the integral action of discrete-time fuzzy ts control under saturated actuator. In *Proc. of the 2018 IEEE Internatoinal Conf. on Fuzzy Systems*, 1596–1603.
- Morato, M.M., Mendes, P.R.C., Normey-Rico, J.E., and Bordons, C. (2020). LPV-MPC fault-tolerant energy management strategy for renewable microgrids. *Int. J. of Electrical Power & Energy Systems*, 117, 105644.
- Pandey, A.P. and de Oliveira, M.C. (2017). A new discrete-time stabilizability condition for Linear Parameter-Varying systems. *Automatica*, 79, 214–217.
- Ruiz, A., Rotondo, D., and Morcego, B. (2019). Design of state-feedback controllers for linear parameter varying systems subject to time-varying input saturation. *Applied Sciences*, 9(17), 3606.
- Senname, O., Dugard, L., Gaspar, P., et al. (2019). \mathcal{H}_∞ /LPV controller design for an active anti-roll bar system of heavy vehicles using parameter dependent weighting functions. *Heliyon*, 5(6), e01827.
- Sousa, A.C., Leite, V.J.S., and Rubio Scola, I. (2018). Affordable Control Platform with MPC Application. *Studies in Informatics and Control*, 27(3), 265–274.
- Tarbouriech, S., Garcia, G., Gomes da Silva Jr., J.M., and Queinnec, I. (2011). *Stability and stabilization of linear systems with saturating actuators*. Springer.
- Yamamoto, K., Senname, O., Koenig, D., and Moulairé, P. (2019). Design and experimentation of an LPV extended state feedback control on electric power steering systems. *Control Engineering Practice*, 90, 123–132.